Bioresource Technology 209 (2016) 100–107

Contents lists available at ScienceDirect

Bioresource Technology

journal homepage: www.elsevier.com/locate/biortech

Distribution patterns of nitrogen micro-cycle functional genes and their quantitative coupling relationships with nitrogen transformation rates in a biotrickling filter

Honglei Wang [a,b], Guodong Ji [b,*], Xueyuan Bai [c]

[a] Institute of Soil and Water Conservation, Northwest A&F University, Yangling 712100, Shaanxi, China
[b] Key Laboratory of Water and Sediment Sciences, Ministry of Education, Department of Environmental Engineering, Peking University, Beijing 100871, China
[c] State Environmental Protection Key Laboratory of Wetland Ecology and Vegetation Restoration, School of Environment, Northeast Normal University, Changchun 130117, China

HIGHLIGHTS

- Distribution patterns of N functional genes were quantitatively assessed.
- N functional genes enriched in different depth gradients of the biofilter.
- DNRA coupled with nitrification and denitrification was a pathway for N removal.
- *Nas* showed a negative relationship with NH_4^+ removal and NO_3^- accumulation.

GRAPHICAL ABSTRACT

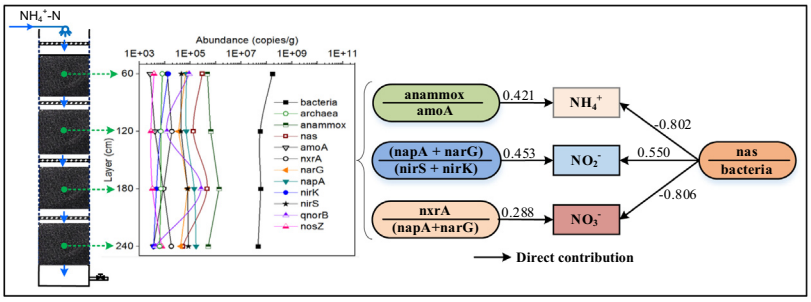

ARTICLE INFO

Article history:
Received 19 December 2015
Received in revised form 23 February 2016
Accepted 25 February 2016
Available online 3 March 2016

Keywords:
Biofilter
Distribution pattern
Nitrification
DNRA
Quantitative relationship

ABSTRACT

The present study explored the distribution patterns of nitrogen micro-cycle genes and the underlying mechanisms responsible for nitrogen transformation at the molecular level (genes) in a biotrickling filter (biofilter). The biofilter achieved high removal efficiencies for ammonium (NH_4^+-N) (80–94%), whereas nitrate accumulated at different levels under a progressive NH_4^+-N load. Combined analyses revealed the anammox, *nas*, *napA*, *narG*, *nirS*, and *nxrA* genes were the dominant enriched genes in different treatment layers. The presence of simultaneous nitrification, ammonium oxidation (anammox), and dissimilatory nitrate reduction to ammonium (DNRA) were the primary factors accounted for the robust NH_4^+-N treatment performance. The presence of DNRA, nitrification, and denitrification was determined to be a pivotal pathway that contributed to the nitrate accumulation in the biofilter. The enrichment of functional genes at different depth gradients and the multi-path coupled cooperation at the functional gene level are conducive to achieving complete nitrogen removal.

1. Introduction

The long-term intensive application of nitrogen (N) fertilizer in China has caused the contamination of surface waters (e.g., rivers, lakes, and reservoirs). Water bodies in China have been seriously polluted since the 1990s, and there have been no marked improvements in recent years (Sun et al., 2012). China has 4880 lakes, covering a total area of 83,400 km^2 and accounting for 0.8% of the country's land area. According to an evaluation of eutrophication in 121 major lakes in 2014, approximately 76.9% of the lakes were eutrophic (MWR, 2014). These lakes serve as China's main sources of drinking water. High levels of ammonium (NH_4^+-N) and nitrate (NO_3^--N) in drinking water are also concerns for human health

* Corresponding author. Tel.: +86 1062755914/87.
E-mail address: jiguodong@pku.edu.cn (G. Ji).

http://dx.doi.org/10.1016/j.biortech.2016.02.119
0960-8524/

because they can poison infants by provoking methemoglobinemia (David et al., 2013). Thus, polluted drinking water must be pretreated to remove excess NH_4^+-N and NO_3^--N.

Biotrickling filter (biofilter) systems have been engineered and intensively studied as a sustainable technology for improving drinking water. Biofilters have attracted considerable interest due to the well-established advantages of these systems, such as simple design and operation, low capital and operating costs and a low requirement for energy and maintenance inputs (Van den Akker et al., 2011; Wang et al., 2015a; Wik, 2003). In a biofilter, water is distributed over a tower containing the packed media. Then, as the water trickles down, microorganisms in the biofilm degrade nitrogen via several ecological processes, such as nitrification, denitrification, and anaerobic ammonium oxidation (anammox) (Ji et al., 2012b; Wang et al., 2015b). Microbial communities exhibit substantial heterogeneity in their spatial distributions (Andrus et al., 2014). Furthermore, these differences in spatial distribution can have a considerable effect on nitrogen removal in biofilters (Ji et al., 2013); thus, investigations of the spatial distribution patterns of microbial communities can provide insight into processes mediated by microbes. The distribution patterns of the microbial community were related to the water flow and showed increased diversity with decreasing nutrient levels and increasing water residence times (David et al., 2013). An analysis of the spatial and temporal distribution of ammonia monooxygenase (*amoA*) and nitrous oxide reductase (*nosZ*) in a pilot-scale biofilter indicated that ammonia-oxidizing and denitrifying bacteria coexisted in both the anoxic and aerated areas (Gómez-Villalba et al., 2006). As noted by Gilbert et al. (2008), denitrifiers were mainly enriched near the surface of the filter, and a microbiological gradient was present along the water flow. Juhler et al. (2009) studied the abundance distribution of *amoA* in a biofilter. The results showed that the absolute abundance of the ammonium oxidation gene *amoA* was low at the biofilter outlet. Ji et al. (2013) investigated the spatial distribution of nitrogen removal functional genes in multimedia biofilters for sewage treatment. The results showed that anammox bacterial 16S rRNA (anammox) and the other nitrogen removal functional genes all were dominantly enriched at different depth gradients. Anammox, periplasmic nitrate reductase (*napA*), nitric oxide reductase (*qnorB*), and *nosZ* showed partially or mutually beneficial cooperation. The nitrite oxidoreductase (*nxrA*) and nitrite reductase (*nirK*) genes showed protocooperation, and the *amoA* and *narG* genes showed partially beneficial cooperation. The dissimilatory nitrate reduction to ammonium (DNRA) process has been described in many systems, including tropical forest soils, freshwater sediments, marine environments, coastal ecosystems, and constructed wetlands (Brunet and Garcia-Gil, 1996; Giblin et al., 2013; Silver et al., 2001; Zhi et al., 2015). The nitrate reduction coding gene *nas* is often regarded as a marker of the DNRA process (Canfield et al., 2010). DNRA, coupled with anammox and ammonia oxidation, was determined to be a pivotal pathway that contributed to NH_4^+-N and NO_3^--N removal, which is similar to a recent study that first reported that co-occurring anammox and DNRA were responsible for the intensive nitrogen loss in tidal flow constructed wetlands (Zhi et al., 2015). The DNRA process, which has been ignored in the field of biofilters to date, may be an important pathway contributing to NO_3^--N removal in biofilters and may rival denitrification in terms of its importance and contribution to the nitrogen balance.

However, few studies on DNRA in biofilters have been reported, and thus little is known about the fate of nitrogen after its transformation from NO_3^--N to NH_4^+-N via DNRA. To date, only a few studies focusing on the distribution patterns of nitrogen micro-cycle functional genes have been published, and very little is known about the DNRA process in biofilters. The lack of a quantitative link between transformation rates of NH_4^+-N and NO_3^--N and *nas* functional gene limits the ability to optimize NH_4^+-N removal and reduce NO_3^--N accumulation to reliably predict long-term effluent quality.

The overall goal of the current study was to analyze the spatial distribution of nitrogen functional genes and understand the effects of DNRA, nitrification, denitrification, and anaero ammonium oxidation (anammox) processes at the molecular level in a controlled biofilter. The following four specific objectives were pursued: (1) evaluation of the treatment performance of NH_4^+-N and NO_3^--N removal; (2) quantitative analysis the spatial distribution of functional genes involved in nitrogen removal; (3) investigation of the respective key functional genes and primary nitrogen removal pathways at different depth gradients; and (4) determination of the quantitative coupling relationships between the nitrogen transformation processes and functional genes.

2. Methods

2.1. Biotrickling filter

One laboratory-scale biofilter with dimensions of 40 cm (length) × 30 cm (width) × 240 cm (depth) (working volume of 144 L) was built (see Fig. S1 In Supplementary Information). The biofilter consisted of four treatment layers (from top to bottom: 20–60 cm, 80–120 cm, 140–180 cm, and 200–240 cm). The four treatment layers were filled with polyurethane foaming plastic with a porosity factor of 75–90%. A sieve tray was installed between each treatment layer. Forty-eight holes were evenly drilled into each sieve tray to allow for contact between the wastewater and air. The biofilter was fed with NH_4^+-N wastewater to investigate the treatment performance treating contaminated lake water. The Chemical Oxygen Demand (COD) concentration in the lake section investigated ranged from 6.0 to 25 mg/L, and the NH_4^+-N concentration in the lake section investigated ranged from 1.2 to 15 mg/L. Synthetic wastewater (see Table S1 in the Supplementary Information) was derived from Beijing groundwater, in which the NO_3^--N concentration varied from 4.9 to 5.0 mg/L throughout the study (35 week). 0.006–0.024 g glucose and 0.004–0.045 g NH_4Cl per liter were added to tap water, resulting in concentrations of 6.0–25.0 mg/L COD and 1.2–15.0 mg/L NH_4^+-N. The hydraulic loading rate was maintained at 2.0 $m^3/m^2/d$. The synthetic wastewater was prepared daily in a feeding tank and then pumped into the top treatment layers. The immobilized B350M microorganisms, which purchased from BIO-SYSTEMS Co. (USA) (Ji et al., 2012a), were placed in the four treatment layers. 40 g of B350M microorganisms was placed in each treatment layer. The biofilter was placed indoors, and influents and effluents ranged in temperature from 10.3 to 26.9 °C. The experiment began on December 28, 2012 and involved the following six stages (total 35 weeks): start-up stage (0–14 week) from December 28 to February 23; stage I (15–19 week) from February 24 to March 29; stage II (20–23 week) from March 30 to May 3; stage III (24–27 week) from May 4 to June 7; stage IV (28–31 week) from June 8 to July 12; and stage V (32–35 week), from July 13 to August 16.

2.2. Sample collection and determination

Water samples were collected from the biofilter nine times (start-up stage) and three times during each operational stage. The water samples were analyzed immediately at the Key Laboratory of Water and Sediment Sciences of Peking University. The dissolved oxygen (DO) content was measured using a DO200 dissolved oxygen meter (YSI, Yellow Springs, Ohio, USA). COD was determined using a HACH DR2800 (HACH, Loveland, Colorado, USA), and the NH_4^+, nitrite (NO_2^-), and NO_3^- were measured using a

UV-1800 spectrophotometer (Shimadzu, Kyoto, Japan). All variables were analyzed according to standard analytical procedures. Microbial samples (including three replicates) were collected from the four treatment layers for a functional gene analysis at the end of weeks 4, 8, 14, 19, 23, 27, 31, and 35. Each layer was extracted at the designed date and then thoroughly mixed to obtain one homogeneous sample for the best representation of the whole treatment layer. Then, the sample was placed in an ice incubator and prepared for subsequent DNA extraction.

2.3. Quantitative polymerase chain reaction (qPCR)

Total genomic DNA from the microbial samples was first extracted and purified using soil DNA kits D5625-01 (Omega Bio-Tek, Norcross, Georgia, USA) and then detected with 1% agarose gel electrophoresis and stored at −20 °C until use. The qPCR technique was employed to investigate the key factors in nitrogen transformation to understand their distribution patterns in the different layers of the biofilter. The absolute abundances of bacterial 16S rRNA (bacterial), archaeal 16S rRNA (*archaeal*), anammox bacterial 16S rRNA (anammox), dissimilatory nitrate reduction to ammonium (*nas*), ammonia monooxygenase (amoA), nitrite oxidoreductase (nxrA), periplasmic nitrate reductase (napA) and membrane-bound nitrate reductase (narG), nitrite reductase (nirK/nirS), nitric oxide reductase (qnorB), and nitrous oxide reductase (nosZ) were quantified on a MyiQ2 Real-Time PCR Detection System (Bio-Rad, USA). The primers for each target gene are presented in Supplementary Table S2.

2.4. Data analysis

The influent and effluent concentrations of COD, NH_4^+-N, NO_2^--N, and NO_3^--N along with the hydraulic retention time (HRT = 1.7 h) were used to calculate the removal efficiencies (%) and nitrogen transformation rates. The absolute abundances of bacterial, *archaeal*, and functional genes (i.e., anammox, *nas*, *amoA*, *nxrA*, *narG*, *napA*, *nirK*, *nirS*, *qnorB*, and *nosZ*) were averaged and then used as basic candidate variables in stepwise regression analyses (SPSS 20, U.S.A.) to obtain correlations with the nitrogen transformation rates (Wang et al., 2015a; Zhi et al., 2015).

3. Results and discussion

3.1. Nitrogen Removal and Transformation

The influent and effluent concentrations of NH_4^+-N, NO_2^--N, NO_3^--N and TN and their transformation rates during different operation periods are shown in Fig. 1. During the operation stage (weeks 15–35), the NH_4^+-N effluent concentration fluctuated between 0.3 and 1.5 mg/L (removal efficiencies ranging from 80.0% to 95.8%), with a progressive NH_4^+-N removal loading rate ranging from 15.2 to 192.3 g/m^3/d. The average NO_2^--N effluent concentration gradually increased from 0.3 mg/L in the start-up stage (weeks 0–14) to 3.2 mg/L in stage V (weeks 32–35), with a NO_2^--N accumulation rate ranging from 2.8 to 47.5 g/m^3/d. The average TN effluent concentration fluctuated between 5.0 and 6.0 mg/L in the start-up stage (weeks 0–14), with a TN removal loading rate ranging from 0.2 to 16.1 g/m^3/d. During the operation stage (weeks 15–35), the average TN effluent concentration fluctuated between 0.8 and 8.8 mg/L, with a TN removal loading rate ranging from 10.8 to 124.1 g/m^3/d. The synthetic wastewater used in this study was derived from Beijing groundwater, in which the NO_3^--N effluent concentration fluctuated between 4.9 and 5.0 mg/L during the start-up stage and operation stage. During the start-up stage and stage I (weeks 15–19), the NO_3^--N effluent concentration fluctuated between 4.6 and 4.9 mg/L. However, the NO_3^--N effluent concentration increased sharply from 5.3 to 12.1 mg/L during the remaining operation periods (weeks 20–35), with the NO_3^--N accumulation rate ranging from 12.3 to 93.7 g/m^3/d (Fig. 1). As noted by Pang et al. (2015), NO_3^--N accumulation in different systems (e.g., biofilters or constructed wetlands) was attributed to limited denitrification processes, which were believed to be the only significant mechanism of NO_3^--N removal. This limitation in NO_3^--N removal mechanisms might be due to insufficient carbon sources for denitrification as organic carbon was preferentially degraded. Denitrification is primarily performed by heterotrophic nitrifying bacteria that use organic carbon as an energy source and require an appropriate C/N ratio (C/N > 6) to function properly (Wang et al., 2015a; Zhi and Ji, 2014). In the present study, the C/N ratio decreased from 5.0 (weeks 20–23) to 1.7 (weeks 32–35) (Table 1), leading to a lack of sufficient organic carbon and potentially causing an increase in NO_3^--N accumulation in the system. Previous studies have also reported that the DNRA played an important role in NO_3^--N removal in many systems (Giblin et al., 2013; Silver et al., 2001; Zhi et al., 2015).

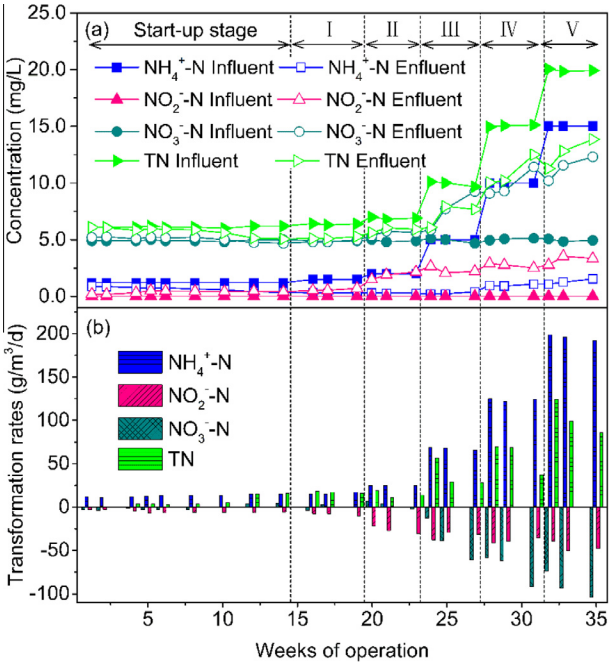

Fig. 1. Nitrogen levels of the influent and effluent (a) and long-term dynamic transformations (b).

3.2. Distribution patterns of nitrogen functional genes

The absolute abundances of bacterial, *archaeal*, anammox, *nas*, *amoA*, *nxrA*, *narG*, *napA*, *nirK*, *nirS*, *qnorB*, and *nosZ* genes in the four treatment layers (from top to bottom: 20–60 cm, 80–120 cm,

Table 1
Quantitative relationships between nitrogen transformation rates and functional gene groups with unstandardized coefficients (n = 8).

Stepwise regression models (equations)	R^2	P value
NH_4^+-N = 0.039 anammox/amoA − 8228.453 nas/bacteria + 125.265	0.998	0.001
NO_2^--N = 2.848 (napA + narG)/(nirS + nirK) + 698.701 nas/bacteria − 47.316	0.912	0.044
NO_3^--N = −4351.270 nas/bacteria + 39.279 nxrA/(napA + narG) + 67.846	0.984	0.008

140–180 cm, and 200–240 cm) were quantified eight times (weeks 0–35, see Figs. S2 and S3 in the Supplementary Information). The absolute abundances of nitrogen functional genes in the four treatment layers were averaged and then used to determine the overall distribution patterns (Fig. 2) in the biofilter during the experimental period.

The results from Fig. 2(a) show that the abundance of bacteria and *archaea* gradually declined along the water direction (from top to bottom). The average abundance of bacteria in the four treatment layers was 8.3×10^7 copies/g. The abundance of bacteria decreased slightly from 1.7×10^8 copies/g in the 20–60 cm layer to 4.6×10^7 copies/g in the 200–240 cm layer. The average abundance of *archaea* in the four treatment layers was 7.0×10^3 copies/g. Copies of *archaea* decreased from 8.0×10^3 copies/g in the 20–60 cm layer to 6.2×10^3 copies/g in the 200–240 cm layer, showing late emergence and low initial abundance. The standard curve of archaeal 16S rRNA used in this study ranged from 1.0×10^2 to 1.0×10^6 copies/g with $R^2 = 0.992$, leading to precise quantification robust to measurement errors. Although archaea were not dominant in the microbial community in the four treatment layers, these minor members of the microbial community may play pivotal roles in transformation and removal in the biofilter (Angnes et al., 2013; Zhi et al., 2015).

The abundance of *amoA*, *nxrA*, and anammox, which are the three functional genes involved in NH_4^+-N transformation, are summarized in Fig. 2(a). The anammox exhibited a similar spatial variation trend with the amoA gene along the water direction. The absolute abundance of anammox and *amoA* genes reached a peak in the 140–180 cm layer. The abundances of anammox and *amoA* in this layer (140–180 cm) were 1.4×10^7 and 8.6×10^3 copies/g, which were 2.9 and 3.3 times greater than those in the 20–60 cm layer, respectively. The average abundance of anammox in the four layers was 157 times greater than that of *amoA*, thereby promoting the anammox process as the dominant NH_4^+-N removal pathway. One possible explanation for this result is that DO was primarily consumed in the oxidation of substantial organic matter (80–96% COD removal) during different operation stages, which created increasingly anaerobic environmental conditions favorable for the growth and enrichment of anammox bacteria as the major driver of NH_4^+-N and NO_2^--N removal. Previous studies investigated that the optimum growth pH for anammox is 6.7–8.3, and its optimum growth temperature is 20–43 °C (Marc Strous et al., 2006). Both the pH (7.8–8.4) and temperature (18–25 °C) (see Fig. S4a, b in the Supplementary Information) of the influent and effluent of the biofilter benefit the growth and enrichment of anammox bacteria. The ammonia monooxygenase coding gene *amoA* is considered the rate-limiting step of aerobic ammonia oxidation and is also the central link of nitrogen removal (Dionisi et al., 2002). The results in Fig. 2(a) shows that the absolute abundance of *amoA* close to the outlet (the 200–240 cm layer) in the biofilter was lower than those in the other layers, supporting the previous assessments that the abundance of *amoA* at the outlet of a biological filter is lower due to the competition for oxygen by heterotrophic bacteria (Juhler et al., 2009). A previous study also found that while determining suitable pH, DO, and NH_4^+-N concentrations, a higher NH_4^+-N concentration enhanced the growth of aerobic AOB (Rothrock et al., 2011). In this study, both the pH values (7.8–8.4) and DO concentrations (5.5–10.6 mg/L, see Fig. S4c in the Supplementary Information) of the influent and effluent of the biofilter were in a suitable range for the growth of ammonia oxidizing bacteria (AOB) (Ji et al., 2013). The NH_4^+-N concentration decreased along the water direction, which could be the main reason why the abundance close to the outlet (the 200–240 cm layer) was lower than those in the other layers of the biofilter. In addition, the *amoA* and anammox genes exhibited an associated fluctuating distribution along the water direction because anammox was dependent on the NO_2^--N produced from ammonia oxidation performed by the *amoA* gene. The nitrite oxidase coding gene *nxrA* is a key gene for nitrite oxidizing bacteria (NOB) to oxidize NO_2^--N to NO_3^--N. As shown in Fig. 2(a), the abundance of *nxrA* fluctuated mildly in the four treatment layers, ranging from 8.6×10^3 to 1.8×10^4 copies/g. Yan et al. (2003) reported that the growth of nitrite-oxidizing bacteria (NOB) was promoted when dissolved oxygen (DO) is more than 3.0 mg/L. In our case, the DO concentrations in the biofilter ranged from 5.5 to 10.6 mg/L, which was favorable for the enrichment and growth of NOB in the four treatment layers. This intensified DO was largely attributed to the enhanced oxygen supply generated by the sieve tray operation to allow for the wastewater/air contact.

The *nas* gene exhibited slight fluctuations along the water direction (Fig. 2(a)), reaching their nadirs (5.0×10^4 copies/g) in the 200–240 cm layer. The lowest absolute abundance of *nas* near the 200–240 cm layer may be related to DO (range 5.5–10.6 mg/L) in excess of the activity inhibition partial pressure of oxygen. Fig. 2a indicates that the *nas* gene exhibited a similar trend in spatial variation with the anammox gene. This associated fluctuating pattern between the *nas* and anammox genes was due to similar environmental adaptations (anaerobic condition) and ecological interactions between anaerobic ammonium oxidation bacteria (anammox) and DNRA bacteria (*nas*) (Ji et al., 2012b). The *nas* gene performs NO_3^--N to NH_4^+-N oxidation, providing intermediate product (NO_2^--N) to anammox for the ammonium oxidation of NH_4^+-N to N_2. This might also explain the corresponding lower abundance of the *nas* gene than the anammox gene. These coupled multipath interactions and the presence of the anammox gene are believed to favor complete NH_4^+-N removal in the biofilter.

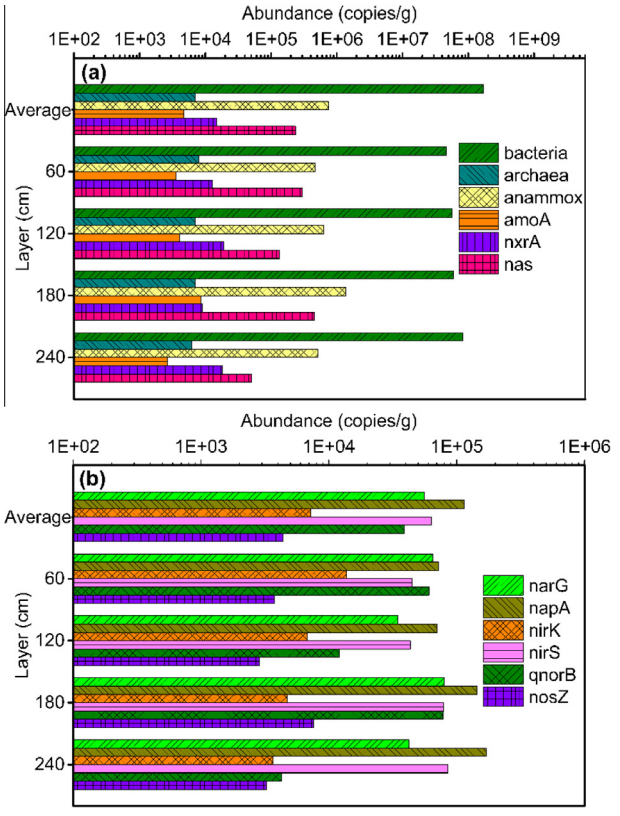

Fig. 2. Absolute abundance of microbial communities and functional genes: bacterial and archaeal 16S rRNA, anammox 16S rRNA, *amoA*, *nxrA*, and *nas* (a); *narG*, *napA*, *nirK*, *nirS*, *qnorB*, and *nosZ* (b).

Denitrification was long believed to be the only significant mechanism in nitrate removal (Lina et al., 2002). However, the average absolute abundance of *nas* in the four treatment layers was 3.8 and 2.4 times greater than the nitrate reductase genes *napA* and *narG*, respectively (Fig. 2(a, c)), suggesting that DNRA may be a pivotal pathway for NO_3^--N removal (Rütting et al., 2011).

Six denitrifying genes, *napA*, *narG*, *nirK*, *nirS*, *qnorB*, and *nosZ*, are summarized in Fig. 2(b). The *napA* gene had a significantly higher (2.3-fold) abundance than the counterpart *narG* gene, similar to other studies reporting that the *napA* gene was dominant under anoxic conditions and the *narG* gene was dominant under anaerobic conditions. Patureau et al. (2000) found that when the DO concentration was less than 4.5 mg/L, the aerobic denitrification rate increased with increasing DO. In this study, the increase in DO (5.5–10.6 mg/L) in the effluent enhanced the growth of aerobic denitrifying bacteria, indicating that DO was a key factor for the enrichment of *napA* in the 200–240 cm layer. Based on the results of *amoA* and anammox (Fig. 2(a)), the abundance of amoA is largely lower than anammox. The first step of nitrification (NH_4^+-N → NO_2^--N) may not be the main pathway for NO_2^--N substrate supply to anammox. The abundance of (*napA* + *narG*) (1.7×10^5 copies/g) exhibited nearly equal abundance compared to anammox (7.46×10^5 copies/g).The (*napA* + *narG*) and anammox showed an associated fluctuating distribution along the water direction. The results demonstrated that simultaneous nitrification, denitrification, and anammox (SNAD) processes were confirmed at the molecular level in the biofilter. The co-existence of SNAD processes can assist in the simultaneous removal of nitrogen and organic carbon in the system, rather than a sequential chain of treatments (Lan et al., 2011; Wang et al., 2015a). The *nirS* gene had a significantly higher abundance (12.4-fold) than the counterpart *nirK* gene in four layers, similar to other studies reporting that the *nirS* gene was environmentally more abundant than the *nirK* gene (Kandeler et al., 2006). Higher *nirS* gene abundance indicated that it not only played a dominant role in nitrite reduction but was also a primary contributor to the production of the greenhouse gas NO in the biofilter. Ruiz et al. (2003) found that the optimal DO concentration for the denitrifying bacterial community is 1.0–1.5 mg/L. The influent and effluent DO concentrations in the system do not benefit the growth and enrichment of denitrifying bacteria. The absolute abundances of *qnorB* and *nosZ* genes exhibited similar fluctuations and reached their peaks in the 180 cm layer because the main product of denitrification catalyzed by *nirK* codase and *qnorB* codase was N_2O. The reaction catalyzed by *nosZ* codase used N_2O as a substrate, namely, the reactions catalyzed by *nirK* codase and *qnorB* codase were both conducive to the enrichment of *nosZ* functional gene communities (Bell et al., 1990). In this study, *nirK* was relatively enriched in the 240 cm layer, the N_2O released from the denitrification process catalyzed by *nirK* codase migrates against the water direction, and this migration was conducive to the relative enrichment of *nosZ* in the 140–180 cm layer. In addition, *qnorB* was also relatively enriched in the 140–180 cm layer. NO reductase, encoded by the *qnorB* gene, has a high affinity for NO, and it preferentially employs electrons into the process in which NO is deoxidized to N_2O (Fujiwara and Fukumori, 1996), which will also increase the relative enrichment of *nosZ* gene communities in the same layer (140–180 cm layer).

3.3. Nitrogen transformation pathway

Following the descriptive characterization of the roles and distribution patterns of nitrogen functional genes, the next objective was to discern and compare the primary nitrogen removal pathways during different stages. Results from Fig. 1(b) showed NH_4^+-N removal rate and NO_2^--N accumulation rate noticeably increased during stage II (20–23 week) to stage V (32–35 week). Therefore, the functional genes data from stage II and stage V were combined to compare the nitrogen transformation pathways that determine the treatment performance of NH_4^+-N removal and NO_3^--N accumulation. The relative richness of nitrogen functional genes were defined as the percentage of absolute abundance of a nitrogen functional gene in a layer/absolute abundance of all nitrogen transfer genes in this layer. The nitrogen transformation process and pathway were classified into three groups according to the relative richness value. The main pathway was defined as the relative richness value more than 10%; the secondary pathway was defined as the relative richness value between 5% and 10%; the restricted pathway was defined as the relative richness value less than 5%.

The nitrogen transformation processes and pathways in different layers during stage II (weeks 20–23) are shown in Fig. 3. The main pathways in the 20–60 cm layer were anammox and DNRA, and the secondary pathway was the first step of denitrification (NO_3^--N → NO_2^--N). The main pathway in the 80–120 cm layer was anammox, and the secondary pathways were DNRA and the first step of denitrification. The main pathways in the 140–180 cm layer were anammox and DNRA. The main pathway in the 200–240 cm layer was anammox, and the secondary pathways were DNRA and the second step of denitrification (NO_2^--N → NO). In the four layers (20–60 cm, 80–120 cm, 140–180, and 200–240 cm), the restricted pathway is nitrification, the third step of denitrification (NO → N_2O) and the fourth step of denitrification (N_2O → N_2). The results from Fig. 3 indicated that the anammox functional gene was predominantly enriched in the four layers, resulting in the robust NH_4^+-N and NO_2^--N removal performance during stage II. The predominant enrichment of DNRA bacteria (*nas* gene) and NO_3^--N oxidation bacteria (*napA*, and *narG* genes) were the primary reasons for the NO_3^--N removal performance in the 20–60 cm and 80–120 cm layers, suggesting an overall low NO_3^--N accumulation rate in the biofilter.

The nitrogen transformation processes and pathways in the different layers during stage V (weeks 32–35) are shown in Fig. 4. The main pathways in the 20–60 cm layer were anammox and DNRA, and the secondary pathway was the first step of denitrification. The main pathway in the 80–120 cm layer was anammox, and the secondary pathways were DNRA and the first and second steps of denitrification. The main pathways in the 140–180 cm layer were anammox and the second and third steps of denitrification. The main pathways in the 200–240 cm layer were the first and second steps of denitrification and the second step of nitrification (NO_2^--N → NO_3^--N), and the secondary pathway was anammox. The results from Fig. 5 show that the anammox functional gene was predominantly enriched in the four layers, resulting in the robust NH_4^+-N removal performance during stage V. The relative richness of *nxrA* significantly increased in the 200–240 cm layer, suggesting a rapid increase of NO_3^--N production, which also explained the NO_3^--N accumulation in the system during stage V. In addition, the relative richness of *nas* decreased significantly along the layers, suggesting attenuated DNRA activity, which directly decreased the NO_3^--N consumption and NH_4^+-N production in the system during stage V. Based on these results, the layer enrichment (different depth gradients) of functional genes further confirmed that this multi-path coupled cooperation at the functional gene level is also conducive to achieving complete nitrogen removal.

3.4. Quantitative coupling relationships

The multiple regression applied in the study provided a linear quantitative measure of the association of functional genes with nitrogen transformation rates. Path analyses were used to identify key functional genes that determine the nitrogen transformation

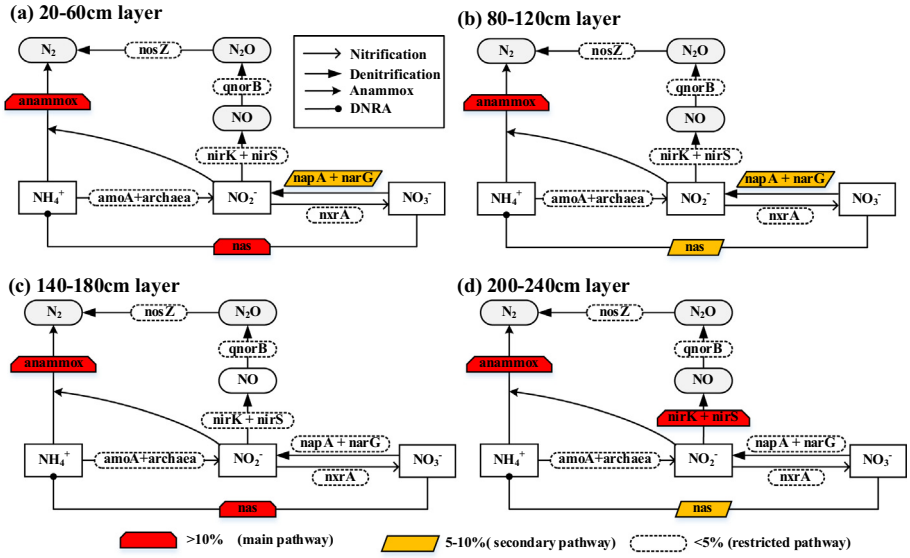

Fig. 3. Nitrogen transformation processes and pathways at different depth gradients during stage II (weeks 20–23). The nitrogen transformation processes and pathways were classified into three groups according to their relative richness values. The main pathway was defined as a relative richness value of more than 10%; the secondary pathway was defined as a relative richness value between 5% and 10%; and the restricted pathway was defined as a relative richness value of less than 5%.

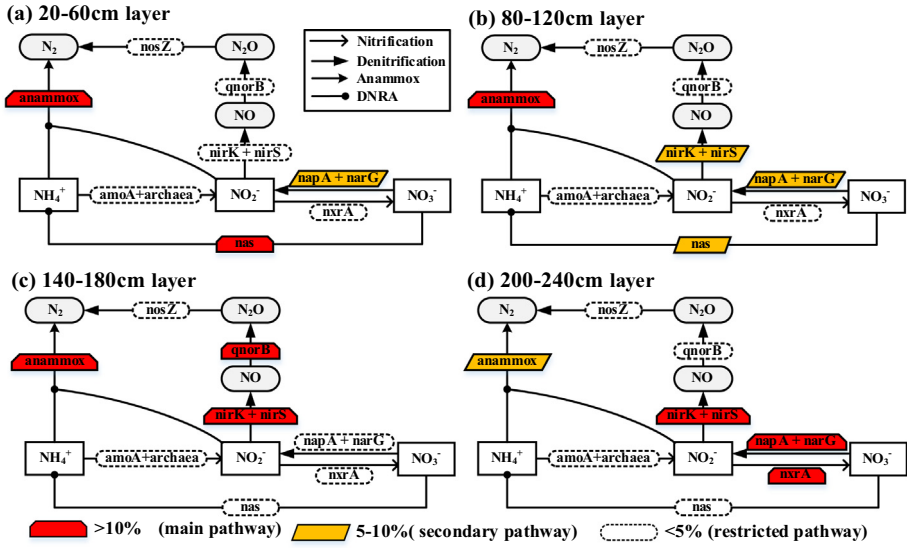

Fig. 4. Nitrogen transformation processes and pathways at different depth gradients during stage V (weeks 32–35). The nitrogen transformation processes and pathways were classified into three groups according to their relative richness values. The main pathway was defined as a relative richness value of more than 10%; the secondary pathway was defined as a relative richness value between 5% and 10%; and the restricted pathway was defined as a relative richness value of less than 5%.

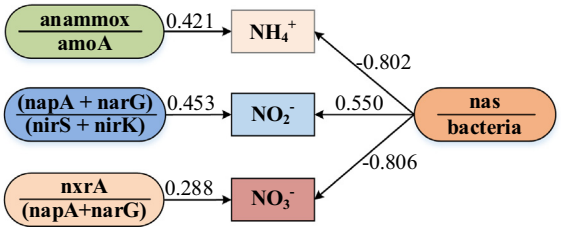

Fig. 5. Path diagrams estimating the direct contributions of functional gene groups to the NH_4^+-N, NO_3^--N, and NO_2^--N transformation rates.

pathways in the biofilter. The results showed that anammox/*amoA* and *nas*/bacteria were responsible for the relationship with the NH_4^+-N transformation rate (Table 1). The first variable, anammox/*amoA*, was directly involved in NH_4^+-N removal in the anaerobic ammonia oxidation and nitrification pathways and was therefore positively correlated with the NH_4^+-N transformation rate. The second variable, *nas*/bacteria, was directly involved in NH_4^+-N production in the DNRA pathway (NO_3^--N → NO_2^--N → NH_4^+-N) and was therefore negatively correlated with the NH_4^+-N transformation rate. The path analysis revealed that the direct positive contribution of anammox/*amoA* to the NH_4^+-N transformation rate was 0.421, and the direct negative contribution of *nas*/bacteria to the NH_4^+-N transformation rate was −0.802 (Fig. 5). The NH_4^+-N transformation rate was collectively determined by the anammox, *amoA*, and *nas* genes. The genes anammox and *amoA* are primarily involved in NH_4^+-N conversion and determine the treatment performance of NH_4^+-N removal in biofilters (Feng et al., 2012; Wang et al., 2015a). The negative quantitative relationship between

nas/bacteria and the NH_4^+-N transformation rate suggested that the less-studied DNRA was an existing but previously underestimated pathway that reduces NH_4^+-N removal in biofilters. The NO_2^--N accumulation rate was numerically determined by *napA*, *narG*, *nirS*, *nirK*, and *nas*. The level of NO_2^--N accumulation is denoted by the ratio of (*napA* + *narG*)/(*nirS* + *nirK*) because *napA* and *narG* genes were directly involved in the production of NO_2^--N, whereas *nirS* and *nirK* genes were responsible for NO_2^--N consumption. The *nas* gene was involved in the medium production of NO_2^--N in the DNRA pathway (NO_3^--N → NO_2^--N → NH_4^+-N). The path analysis revealed that the direct positive contribution of (*napA* + *narG*)/(*nirS* + *nirK*) and *nas*/bacteria were 0.453 and 0.550, respectively (Fig. 5). For NO_3^--N accumulation, *nas*/bacteria and *nxrA*/(*napA* + *narG*) were responsible for the relationship with the NO_3^--N accumulation rate. The first variable, *nas*/bacteria, was directly involved in NO_3^--N transformation in the DNRA pathway and was therefore negatively correlated with the NO_3^--N accumulation rate. The level of NO_3^--N accumulation is denoted by the ratio of *nxrA*/(*napA* + *narG*) because the *nxrA* gene was directly involved in the production of NO_3^--N, whereas the *napA* and *narG* genes were responsible for NO_3^--N consumption. The path analysis revealed that the direct positive contribution of *nxrA*/(*napA* + *narG*) to the NO_3^--N accumulation rate was 0.288, and the direct negative contribution of *nas*/bacteria to the NO_3^--N accumulation rate was −0.806 (Fig. 5). The NO_3^--N accumulation rate was collectively determined by the *nas*, *nxrA*, *narG* and *napA* genes.

4. Conclusions

The biofilter achieved average removal efficiencies of 90% for NH_4^+-N. The anammox, *nas*, *napA*, *narG*, *nirS*, and *nxrA* genes were the dominant enriched genes in different treatment layers. Combined analyses revealed that the presence of simultaneous nitrification, anammox, and DNRA were the primary reasons for the robust NH_4^+-N treatment performance. The results from a stepwise regression analysis suggested that the NH_4^+-N removal rate was collectively controlled by anammox, *amoA*, and *nas*. Specifically, the *nas* gene showed a negative relationship with NH_4^+-N removal and NO_3^--N accumulation.

Acknowledgements

The Key Project of China Spark Program (GL2015007), and the Collaborative Innovation Center for Regional Environmental Quality provided support for this study.

Appendix A. Supplementary data

Supplementary data associated with this article can be found, in the online version, at http://dx.doi.org/10.1016/j.biortech.2016.02.119.

References

Andrus, J.M., Porter, M.D., Rodríguez, L.F., Kuehlhorn, T., Cooke, R.A., Zhang, Y., Kent, A.D., Zilles, J.L., 2014. Spatial variation in the bacterial and denitrifying bacterial community in a biofilter treating subsurface agricultural drainage. Microb. Ecol. 67 (2), 265–272.

Angnes, G., Nicoloso, R.S., Silva, M.L.B.D., de Oliveira, P.A.V., Higarashi, M.M., Mezzari, M.P., Miller, P.R.M., 2013. Correlating denitrifying catabolic genes with N_2O and N_2 emissions from swine slurry composting. Bioresour. Technol. 140, 368–375.

Bell, L.C., Richardson, D.J., Ferguson, S.J., 1990. Periplasmic and membrane-bound respiratory nitrate reductases in *Thiosphaera pantotropha*: the periplasmic enzyme catalyzes the first step in aerobic denitrification. FEBS. Lett. 265 (1), 85–87.

Brunet, R.C., Garcia-Gil, L.J., 1996. Sulfide-induced dissimilatory nitrate reduction anaerobic freshwater sediments. FEMS Microbiol. Ecol. 21 (2), 131–138.

Canfield, D.E., Glazer, A.N., Falkowski, P.G., 2010. The evolution and future of Earths nitrogen cycle. Science 330 (6001), 192–196.

David, C.-G., Germán, T., David, B., Laurent, P., 2013. Spatial distribution of N-cycling microbial communities showed complex patterns in constructed wetland sediments. FEMS Microbiol. Ecol. 83 (2), 340–351.

Dionisi, H.M., Layton, A.C., Harms, G., Gregory, I.R., Robinson, K.G., Sayler, G.S., 2002. Quantification of *Nitrosomonas oligotropha*-like ammonia-oxidizing bacteria and *Nitrospira* spp. from full-scale wastewater treatment plants by competitive PCR. Appl. Environ. Microbiol. 68 (1), 245–253.

Feng, S., Xie, S., Zhang, X., Yang, Z., Ding, W., Liao, X., Liu, Y., Chen, C., 2012. Ammonium removal pathways and microbial community in GAC-sand dual media filter in drinking water treatment. J. Environ. Sci. 24 (9), 1587–1593.

Fujiwara, T., Fukumori, Y., 1996. Cytochrome cb-type nitric oxide reductase with cytochrome c oxidase activity from Paracoccus denitrificans ATCC 35512. J. Bacteriol. 178 (7), 1866–1871.

Giblin, A.E., Tobias, C.R., Song, B., Weston, N., Banta, G.T., Rivera-Monroy, V.H., 2013. The importance of dissimilatory nitrate reduction to ammonium (DNRA) in the nitrogen cycle of coastal ecosystems. Oceanography 26 (3), 124–131.

Gilbert, Y., Le Bihan, Y., Aubry, G., Veillette, M., Duchaine, C., Lessard, P., 2008. Microbiological and molecular characterization of denitrification in biofilters treating pig manure. Bioresour. Technol. 99 (10), 4495–4502.

Gómez-Villalba, B., Calvo, C., Vilchez, R., González-López, J., Rodelas, B., 2006. TGGE analysis of the diversity of ammonia-oxidizing and denitrifying bacteria in submerged filter biofilms for the treatment of urban wastewater. Appl. Environ. Microbiol. 72 (2), 393–400.

Ji, G., Wu, Y., Wang, C., 2012a. Analysis of microbial characterization in an upflow anaerobic sludge bed/biological aerated filter system for treating microcrystalline cellulose wastewater. Bioresour. Technol. 120, 60–69.

Ji, G., Zhi, W., Tan, Y., 2012b. Association of nitrogen micro-cycle functional genes in subsurface wastewater infiltration systems. Ecol. Eng. 44, 269–277.

Ji, G., He, C., Tan, Y., 2013. The spatial distribution of nitrogen removal functional genes in multimedia biofilters for sewage treatment. Ecol. Eng. 55, 35–42.

Juhler, S., Revsbech, N.P., Schramm, A., Herrmann, M., Ottosen, L.D.M., Nielsen, L.P., 2009. Distribution and rate of microbial processes in an ammonia-loaded air filter biofilm. Appl. Environ. Microbiol. 75 (11), 3705–3713.

Kandeler, E., Deiglmayr, K., Tscherko, D., Bru, D., Philippot, L., 2006. Abundance of narG, nirS, nirK, and nosZ genes of denitrifying bacteria during primary successions of a Glacier Foreland. Appl. Environ. Microbiol. 72 (9), 5957–5962.

Lan, C.-J., Kumar, M., Wang, C.-C., Lin, J.-G., 2011. Development of simultaneous partial nitrification, anammox and denitrification (SNAD) process in a sequential batch reactor. Bioresour. Technol. 102 (9), 5514–5519.

Lina, Y.-F., Jinga, S.-R., Wangb, T.-W., Leea, D.-Y., 2002. Effects of macrophytes and external carbon sources on nitrate removal from groundwater in constructed wetlands. Environ. Pollut. 119 (3), 413–420.

Marc Strous, E.P.S.M., Fonknechten, N., Vallenet, D., Segurens, B., Schenowitz-Truong, C., Médigue, C., Collingro, A., Snel, B., Dutilh, B.E., den Camp, H.J.M.O., van der Drift, C., Cirpus, I., van de Pas-Schoonen, K.T., 2006. Deciphering the evolution and metabolism of an anammox bacterium from a community genome. Nature 440 (7085), 790–794.

MWR, 2014. The ministry of water resources of the People's Republic of China (MWR). China Water Res. Bull., <http://wwwmwr.gov.cn/zwzc/hygb/ szygb/qgszygb/201508/t20150828_719423.html>.

Pang, Y., Zhang, Y., Yan, X., Ji, G., 2015. Cold temperature effects on long-term nitrogen transformation pathway in a tidal flow constructed wetland. Environ. Sci. Technol. 49 (22), 13550–13557.

Patureau, D., Bernet, N., Delgenès, J.P., Moletta, R., 2000. Effect of dissolved oxygen and carbon–nitrogen loads on denitrification by an aerobic consortium. Appl. Microbiol. Biotechnol. 54 (4), 535–542.

Rothrock Jr, M.J., Vanotti, M.B., Szögi, A.A., Gonzalez, M.C.G., Fujii, T., 2011. Long-term preservation of anammox bacteria. Appl. Microbiol. Biotechnol. 92, 147–157.

Ruiz, G., Jeison, D., Chamy, R., 2003. Nitrification with high nitrite accumulation for the treatment of wastewater with high ammonia concentration. Water Res. 6 (37), 1371–1377.

Rütting, T., Boeckx, P., Müller, C., Klemedtsson, L., 2011. Assessment of the importance of dissimilatory nitrate reduction to ammonium for the terrestrial nitrogen cycle. Biogeosciences 8 (7), 1779–1791.

Silver, W.L., Herman, D.J., Firestone, M.K., 2001. Dissimilatory nitrate reduction to ammonium in upland tropical forest soils. Ecology 82 (9), 2410–2416.

Sun, B., Zhang, L., Yang, L., Zhang, F., Norse, D., Zhu, Z., 2012. Agricultural non-point source pollution in China: causes and mitigation measures. Ambio 41 (4), 370–379.

Van den Akker, B., Holmes, M., Pearce, P., Cromar, N.J., Fallowfield, H.J., 2011. Structure of nitrifying biofilms in a high-rate trickling filter designed for potable water pre-treatment. Water Res. 45, 3489–3498.

Wang, H., Ji, G., Bai, X., 2015a. Enhanced long-term ammonium removal and its ranked contribution of microbial genes associated with nitrogen cycling in a lab-scale multimedia biofilter. Bioresour. Technol. 196, 57–64.

Wang, H., Ji, G., Bai, X., 2015b. Quantifying nitrogen transformation process rates using nitrogen functional genesin a multimedia biofilter under hydraulic loading rate constraints. Ecol. Eng. 82, 323–329.

Wik, T., 2003. Trickling filters and biofilm reactor modelling. Rev. Environ. Sci. Biotechnol. 2 (2–4), 193–212.

Yan, T.F., Fields, M.W., Wu, L.Y., Zu, Y.G., Tiedje, J.M., Zhou, J.Z., 2003. Molecular diversity and characterization of nitrite reductase gene fragments (nirK and

nirS) from nitrate- and uranium-contaminated groundwater. Environ. Microbiol. 5 (1), 13–24.
Zhi, W., Ji, G., 2014. Quantitative response relationships between nitrogen transformation rates and nitrogen functional genes in a tidal flow constructed wetland under C/N ratio constraints. Water Res. 64, 32–41.
Zhi, W., Yuan, L., Ji, G., He, C., 2015. Enhanced long-term nitrogen removal and its quantitative molecular mechanism in tidal flow constructed wetlands. Environ. Sci. Technol. 49 (7), 4575–4583.